National
Aeronautical
Laboratory

Model Helicopter Rotor Rig and Associated Strain Gauge Balance for Performance Studies

S R PATIL, M A RAMASWAMY
Aerodynamics Division

Technical Memorandum AE 8704

August 1987
Bangalore 560017 India

MODEL HELICOPTER ROTOR RIG AND ASSOCIATED STRAIN GAUGE BALANCE FOR PERFORMANCE STUDIES

PATIL. S. R.[*], & RAMASWAMY. M.A.[**]

ABSTRACT

The details of teetering rotor model and the associated strain gauge balance and calibration fixtures have been presented. Hovering results for 1.22 m diameter teetering rotor model evaluated experimentally have been compared with the simple blade element-momentum theory.

---

* Scientist. Aerodynamics Division

** Professor Indian Institute of Science
Bangalore-560 012

~0,003

NOTATION

a = airfoil lift curve slope, red^{-1}

b number of blades

c = blade chord, m

CdO = section profile drag coefficient

C_f = total skin friction coefficient

section lift coefficient

C_Q rotor shaft torque coefficient, $\frac{Q}{\pi R^3 \rho (AR f R}$

C_T thrust coefficient, $\frac{T}{\pi R^2 .r.R)^3 \rho}$

F.M. = Figure of merit, $0.707 \frac{C_T}{CO}$

I = blade mass moment of inertia, $g\text{-}m^2$

Q torque, kgf-m

R = rotor radius, m

T = Thrust, kgf

induced inflow velocity at rotor, m/sec

X = ratio of blade - element radius to rotor-blade radius (r/R)

blade element angle of attack, measured from line of zero lift., radians

= *Lock number,* $f aCR^4$

® = Collective pitch, radians

,11, _ rotor angular velocity, radians per second

,P = density of air, kg/m^3

tT = rotor solidity, $\frac{be}{7T R}$

Subscripts

i = induced

0 = profile

INTRODUCTION

Experimental investigations using model rotor test rigs have been found to be quite useful in understanding many aspects of the performance of the helicopter rotors (Ref. 1-5). The present study deals with the development of teetering rotor model of diameter 1.22 meter and associated strain gauge balance.

It is also pointed out in Ref. 6 and 7. that the design of rotor strain gauge balance is quite complicated and it is quite different from conventional strain gauge balance. The rotor strain gauge balance will be subjected to the dead weight of the rotor assembly, swesh plate, pitch control mechanism and the load transmitting base plate as shown in Fig.1. This dead weight will be en order of magnitude higher then the aerodynamic lift force acting on the rotor. Therefore this poses some problems in the design. 'It may also be noted that the drag force (axial force) and side force are much smaller compared to lift force, pitching moment and rolling moment. Hence it is necessary to design the balance in such a way that interactions of the pitching moment, rolling moment and lift force on the axial force and the side force elements are minimised. In the present design this has been achieved to some extent by introducing a rigid member between the larger load measuring members and the smaller load measuring members.

Recently it is noted by Alfred Gessow (Ref.8) that the simple blade element-momentum theory predicts the hover performance of helicopter main rotor well within engineering accuracy. This has been confirmed by comparing the present experimental hover results with the theory.

MODEL DESCRIPTION

A photograph off the teetering rotor- model of 1.22 meter diameter with balance and slipring assembly is shown in

Fig.1. A detailed schematic sketch of the same is given in Fig.2. The rotor shaft is driven by a D.C. shunt motor which is rated for a maximum power of 2 HP and 1500 RPM. A speed control unit with closed loop system to regulate the speed with an accuracy of less than it of maximum speed has been used. The speed of the rotor is measured by an electronic tachometer which consists of a photo diode transistor and a disc with sixty equispaced holes to generate sixty pulses per revolution of the rotor. FRP blades with NACA 0012 profile without twist and taper have been attached rigidly to the hub which is mounted on the rotor shaft with a single flap hinge in a teetering or see-saw arrangement. Collective and cyclic pitch on blades can be controlled by means of swash plate which consists of an assembly of rotating and stationary rings, gimball and taper roller bearings as shown in Fig.2. Pitch horn is rigidly attached to the blade and to the pitch link through universal joint in such a way that vertical motion of the link produces pitch motion on the blade. Collctive and cyclic pitch settings on the blades are obtained manually using pitch control mechanism. By the side of the screws which operate the pitch control mechanism, graduated scales are mounted to read the angle settings directly as shown in Fig.2.

Strain gauge torque element is provided on the rotor shaft. Torque singnals from the strain gauge bridge are processed through co-axial type slipring assembly shown in Fig-2.

It is clear from Fig.2, that part of the load experienced by the rotor is transmitted to the shaft and part is transmitted to the swash plate, the total load being fully transferred to the load transmitting base plate. From load transmitting base plate, it is transferred to the balance and then to ground plate. Flexible coupler in the; shaft was provided to transmit only the torque from the motor;

and the axial load directly transmitted through it is negligibly small.

Model Rotor Physical parameters are given 'in the following table.

Diameter	1.22m
Number of blades	2-
Chord	0.05m
Solidity	0.0522
Lock number	1.78
Airfoil section	NACA 0012
Blade taper	None
Blade twist	None

STRAIN-6AU6E BALANCE

A photograph of five components static integral balance with strain gauges attached is shown, in Fig.3. Using the available quick performance evaluation methods which are mainly based on blade element and momentum theory in hovering and forward flight (Ref. 9-11), the loads on the rotor model were calculated. Based on these loads the loads about the balance centre were determined. They are given in the tabular form in Fig.3. An isometric sketch of five components (viz., lift force., drag force, side force, pitching moment, and rolling moment) strain-gauge balance is shown in Fig.4. There are two separate measuring cages, one cage being essentially sensitive to lift, pitching moment and rolling moment and the other cage to axial force and side force. These two cages are separated by a rigid member in order to reduce the interaction of pitching moment, rolling moment and lift force on the axial force and the side force elements. Also the distance between the members which measure the axial and side forces have been kept as large as

possible as shown in Fig.4. Since the design loads are quite small, safety mechanical stops are'provided to protect the balance from over load during fabrication and handling.

The general philosophy that one would like to adopt in the design of the elements, is that the maximum total stress due to all the components of the loads acting simultaneously should roughly be same for all the elements, so that none of the elements becomes either unnecessarily weak or unnecessarily strong. Also one would like to have the full load output for all the components of loads to be same. Further one would like to make the balance as rigid as possible, compatible with the above requirements. It should however be noted that in. practice, these objectives cannot be achieved fully, but the aim should be kept in mind. The detailed design analysis is given in Ref.12.

CALIBRATION FIXTURES

Since the large dead weight of the rotor model is acting on the balance., the static calibration of the balance has been carried out insitu of the rotor model to evaluate its performance. A photograph of the calibration set up for loading the balance in the positive lift force direction is shown in Fig.S. Fig.6, shows the schematic arrangement of the same.. The lift force is applied through a lever arm pivoted at the cehtre using ball bearing as shown in Fig.6. The weight of the lever arm can be balanced using balancing weights. There is a provision in the rig for longitudinal and lateral movement adjustments such that the lift force can be applied parallel to the shaft axis in one plane which is normal to the base. Loading for lift force in negative direction can be carried out by placing standard weights directly on the shaft itself as shown in Fig.7. Fig.8., shows the photograph of calibration set up for pitching moment, rolling moment, drag force and side force. Detailed schematic sketch is given in Fig.9. There are two 'L' shape arms which are pivoted using

ball bearings as shown in Fig.9. The self weights of arms are balanced using balancing weights. There is also a provision in the rig for' adjusting the arm longitudinally and laterally so that pure drag force and side force can be applied.. Friction measured in all these calibration fixtures was in the order of 2-3 grammes.

Torque element fabricated in the rotor shaft has been gauged and calibrated using the separate experimental set up as shown in photograph (Fig-10).. During calibration the strain gauge bridge is excited with constant D.C. **supply of** 3 volts and signals from the bridge are recorded using a DVM of 1 microvolt resolution and amplifier with built in filters with 1000 gain.

Typical calibration curves for lift force and torque are shown in Figs.11 & 12 respectively. The linearity of the curves shows that the calibration is quite satisfactory. Lift and torque sensitivities required for hovering data evaluation were determined from these curves.

TEST PROCEDURE

After calibration, without disturbing the rotor model assembly, hover tests were conducted on 1.22 m dia teetering rotor model. Fig.13 shows a view of **the experimental set** up. Instruments used during tests were, **speed** controller with feed back system, D.C. power supply unit to supply constant excitation voltage to the strain gauge bridges, D.V.M. with one microvolt resolution, oscillograph recorder to observe the AC & DC signals separately to ensure low level of vibrations during experiments, amplifiers with 1000 gain, with built in filters which have the capacity of filtering A.C. signals upto 1 Hz. Fig.13 shows a photograph of these instruments. After sufficient warm up time for the lubricating oil pressure to stabalize, tare thrust and torque readings were obtained without blades on the hub at two typical speeds. At the same speeds with blades installed on

the hub for zero collective pitch setting on the blades the thrust and torque readings were obtained. This was repeated for different collective pitch settings on the blades in steps of 1° upto 5° and in steps of 0.5° upto 8°. Absloute values of thrust and torque were evaluated by correcting for tare values.

COMBINED BLADE ELEMENT AND MOMENTUM THEORY FOR NON-UNIFORM IN FLOW DISTRIBUTION

It has been recently pointed out by Alfred 6essow in Ref.8, that the hover performance prediction using the simple blade element-momentum theory shows good for comparison with experimental data within engineering accuracy. It was therefore felt worthwhile to deal with this theory in some detail, though it is referred in many references (Ref 9 and 10).

The momentum and blade element theories may be combined to derive a general expression for the velocity induced at any point on a helicopter rotor in hovering as given in Ref.9.

From simple blade element theory, the expression for the differential thrust dT on 'b' rotor blade elements operating at a distance 'r' from the axis of rotation and rotating with an angular velocity .t may be written as

$$dT = b \int_{y} (.Ar)^{s} a \left(e - 0 \right) cdr \qquad (1)$$

where

a = airfoil lift-curve slope

e = collective pitch

¢ = in flow.angle, and

P = density of air

An alternative expression for the differential thrust can also be obtained from momentum theory, considering an annular ring of an air screw disc of radius 'r' and width 'dr'. It may be written as

$$dT = 4\pi \rho V^2 r dr \qquad (2)$$

where, V = induced inflow velocity at the location 'r'.

Equating (1) and (2) the expression for the velocity induced can be obtained. Once the induced velocity is known, the inflow angle ϕ = V/A r. at a blade element can be found.

It is given by

$$\phi = \frac{\sigma a}{16 X} + \sqrt{4 + \frac{32}{\sigma a}\frac{B}{X}}$$

where $\sigma = \frac{\text{Total blade area}}{\pi R^2}$, $x = r/R$

With the tip loss factor 'B' the expression for ϕ can be modified to

$$\frac{\sigma a}{16X8}\left(-1 + \sqrt{1 + \frac{32 X8B}{\sigma a}}\right)$$

tip loss factor 'B' is taken to be 0.97 which has generally been found to give good correlation with experimental data (Ref.10).

Now the thrust per unit blade span may be expressed in coefficient form as

$$dC_T/dx = \sigma (a/2)\, aC\, x^2 \qquad (3)$$

where aC = (6- 01

The rotor torque is composed of the induced and profile drag contributions. The induced part, or the torque caused by the components of the lift vectors in the plane of rotation is written as

$$dC_{Q'}/dx = a' (a/2) o \; cc \; x^3 \qquad (4)$$

and the profile drag contribution is

$$dC_{Qp}/dx = (\sigma r/2) C_{d0} x^3 \qquad (5)$$

The profile drag coefficient is determined by the following drag polar given in, Ref.10

$$C_{d0} = C_{dmin} (1 + CL)$$

where the C_{dmin}' the minimum drag coefficient for the airfoil s is given by

$$Cd_{min} = 2C_f (1 + 2 (t/c) + 60 (t/c)^4)$$

where C_f is the skin friction coefficient, t/c is the section thickness ratio. The term 2(t/c) accounts for the velocity increase due t thickness and the term $60(t/c)^4$ is due to the pressure drag given in Ref.10. The skinfriction coefficient C_f can be obtained for the appropriate section Reynolds number from Fig.21.2, of Ref.13.

Then. knowing the geometric and aerodynamic properties of the blade (namely, (T , 0 and 4C) the numerical integrations of equations 3, 4 and 5 have been carried out for the determination of thrust coefficient and torque coefficient.

RESULTS AND DISCUSSIONS

Experiments in hover were conducted on the 1.22 meter diameter rotor model. Thurst and torque were obtained from

the strain gauge balance and the torque element in rotor shaft respectively. Hovering performance evaluation mainly consists of comparing the torque coefficient and figure of merit with thrust coefficient. Figures 14 and 15 show the present experimental- results at Two typical **speeds** of 1200 and 1300 r.p.m. (viz., tip speed a_R = 76.63m/sec., 83.03m/sec.). It is observed from these figures that the agreement of results obtained at these two tip speeds is better than 3%, which is within the experimental error band, except near low values of 9 where setting the blades accurately at small values of 0 is very difficult. Similar observations were made at low values of 8 in Ref.2. The results as expected show that the performance interms of non-dimensional parameters does not depend on the speed.

Comparison of experimental results with theoretical estimates is shown in Figures 16, 17, 18., and 19. It is noted that the drag polar data is absolutely necessary to calculate profile torque coefficient from combined **blade'element and** momentum theory for any rotor. The determination of drag coefficient is based on the estimation of basic skin friction coefficient obtained for the appropriate section Reynolds number. The Reynolds number corresponding to mid span of the blade is 1.63×10^5. Though the Reynolds number is corresponding to laminar flow, the flow on the **blade is** assumed to be turbulent because of the inherent vibration of the blades and consequently, turbulent skin friction data is extra polated to this Reynolds number. The skin friction coefficient for the Reynolds number of 1.63×10^5 was obtained 6.714×10^3 from Ref.13.. corresponding to turbulent flow. With these approximations, it is clearly observed that the agreement between the theoretical estimates and the experimental results for the present rotor is quite good except near low values of 0 as stated earlier. This confirms that the combined blade element and momentum approach works well within engineering accuracy as recently stated by Alfred 6essow in Ref.8.

CONCLUSIONS

Development of experimental techniques using small rotor model is presented in this report. Based on this study, following conclusions have been drawn.

1. The technology involved in development of experimental techniques such as method of transferring rotor loads to balance, design and fabrication of swash plate, method of transferring signals from rotatingpart to stationary part using slip ring assembly, design of flexible coupler, can be easily adapted to the larger size rotor testing facility.

2. Five components, static, integral rotor strain gauge balance which is essentital for full scale rotor testing or flight testing, can be designed and fabricated with associated calibration fixtures to measure mean rotor loads to measuring accuracy.

3. Combined blade element and momentum theory for non-uniform inflow distribution predicts hover performance well within engineering accuracy.

ACKNOWLED6EMENT

The authors sincerely acknowledge Aeronautical Research and Development Board, New Delhi, India for sponsoring this project. Active participation of Mr. K.V.Srikantan and Mr. M.S. Kamaleshiah, in conducting these experiments is acknowledged with thanks.

REFERENCES

1. James, L. Tangier, Robert, M. Wohlfed, and Stan, J. Miley.: "An Experimental Investigation of Vortex Stability, Tip Shapes, Compressibility and Noise for Hovering Model Rotors", NASA-CR-2305., 1974.

2. Walter Castles, JR., Robin, B. Gray.: "Empirical Relation between induced velocity, Thrust, and Rate of descent of a Helicopter Rotor as determined by Wind Tunnel Tests on Four Model Rotors", NACA-TN-2474 October 1951.

3. Lock, C.N.H., Bateman, H., Townend, H.C.H.: "An Extension of the Vortex Theory of Airscrews with applications to Airscrews of Small pitch, including Experimental Results", R & M No 1014, British ARC, 1926.

4. Montgomery, Knight, and Ralph, A. Hefner.: "Static Thrust Analysis of the Lifting Airscrew", NACA-TN-626, December 1937.

5. Henry, R... Velkoff, Thomas, W., Parker.: "Effect of Tip Vanes on the Performance and Flow Field of Rotor in Hover", American Helicopter Society Annual Forum Proceedings, Washington, D.C., May 1982.

6. Victor, M. Ganzer, William, H. Rae.: "An experimental investigation of the effect of Wind Tunnel Walls on the Aerodyamic Performance of a Helicopter Rotor", NASA-TND-415, May 1960.

7. Tadghighi, H., and I.C. Cheeseman.: "Wind Tunnel Investig-ation of High Speed Rotor Noise", Paper No.31 Seventh European Rotorcraft and Powered Lift Aircraft Forum Southampton, U.K. September-,8-11., 1981.

8. Alfred Gessow.: "Understanding and Predicting Helicopter Behaviour - Then and Now", (The Fifth Nikolsky Honorary Lecture presented at the 41st Annual Forum of the American Helicopter Society, Fort Worth, Texas, May 1985) Journal of the American Helicopter Society, Vol 31, No.1, January 1986.

9. Gessow, A.., and Mayers, G.C., Jr.: " Aerodynamics of the Helicopter", Frederick Ungar Publishing Co., New York, 1967.

10. Wayne Johnson.: "Helicopter Theory", Princeton University Press,, Princeton, New Jersey, 1980.

11. Saunders George, H.: Dynamics of Helicopter Flight", John Wiley and Sons Inc., USA, 1975.

12. Ramaswamy, M.A., Patil, S.R., and Raman, K.S.: "Design of Five Component Integral Strain Gauge Rotor Balance", NAL AE-TM-5-83 India, April 1983.

13. Hermann Schlichting.: "Boundary Layer Theory", New York,,; McGraw-Hill Book Co.., Inc., 1960.

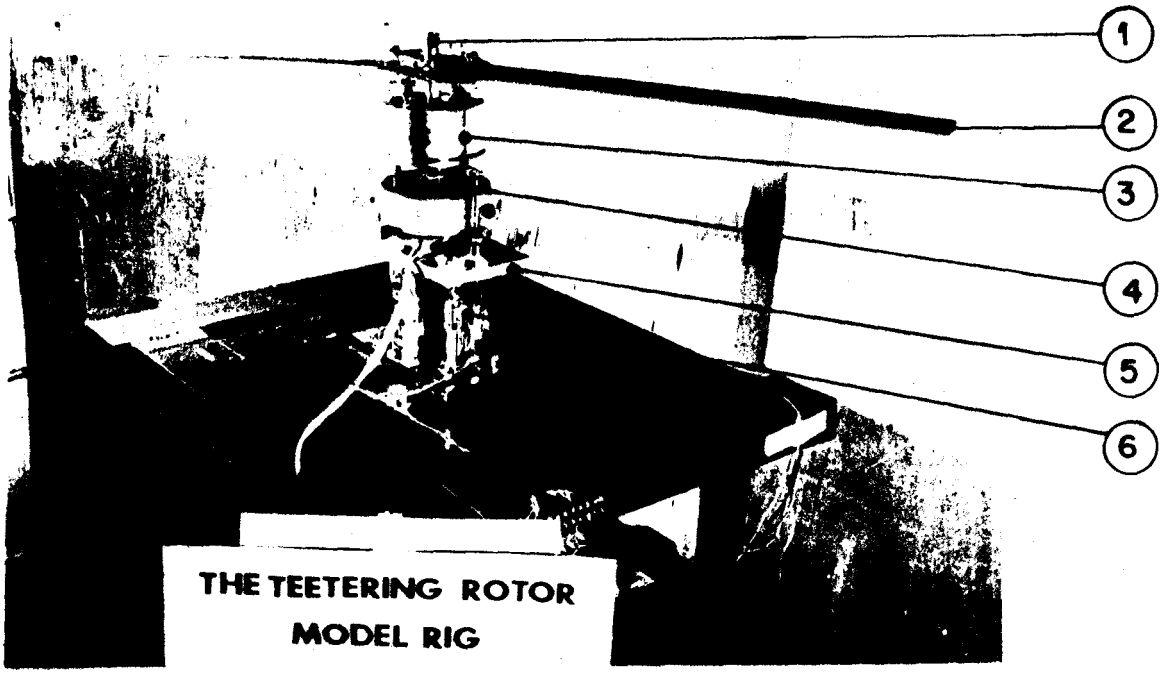

1 . ROTOR SHAFT

2 F. R . P BLADE

SWASH PLATE MECHANISM

4 PITCH CONTROL MECHANISM

5 LOAD TRANSMITTING BASE PLATE

ROTOR BALANCE

FIG.1. ROTOR MODEL WITH BALANCE

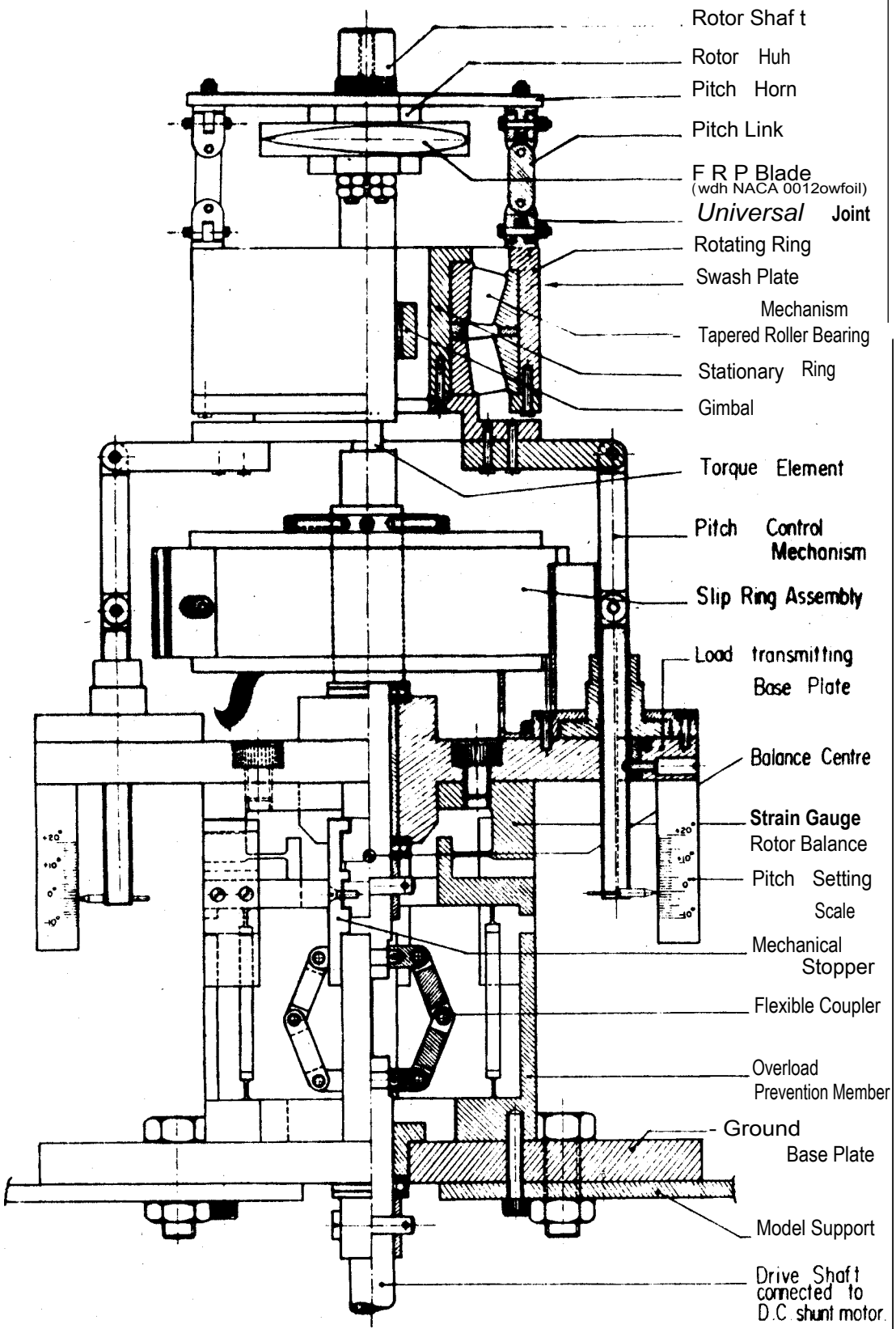

FIG. 2 TEETERING ROTOR MODEL RIG

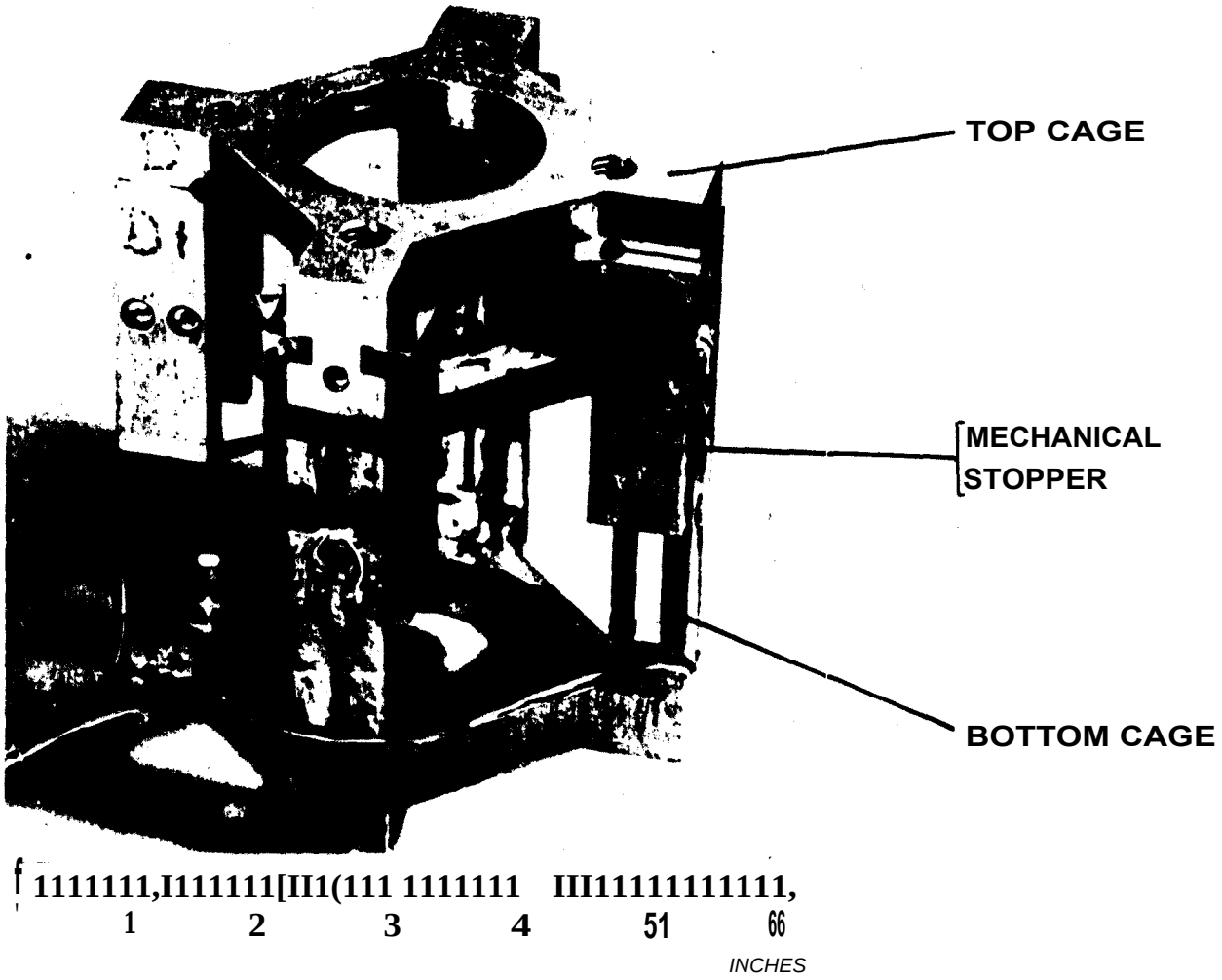

LOAD SPECIFICATIONS

SL. NO.	COMPONENT	MAGNITUDE
1	LIFT FORCE (THRUST)	2 · 730 Kg (**6 lbs-)**
2	AXIAL FORCE (LONGITUDINAL TANGENTIAL FORCE)	0 · 455 Kg (1 lb.)
	SIDE FORCE (LATERAL TANGENTIAL FORCE)	**0** · 1 **36** Kg (0 · 3 lb.)
4	PITCHING MOMENT	107 · 37 **Kg-mm** (9·3 lb-in)
5	ROLLING MOMENT	32 · 10 Kg-mm (2·78 lb-in)

FIG. 3 ROTOR BALANCE AFTER GAUGING

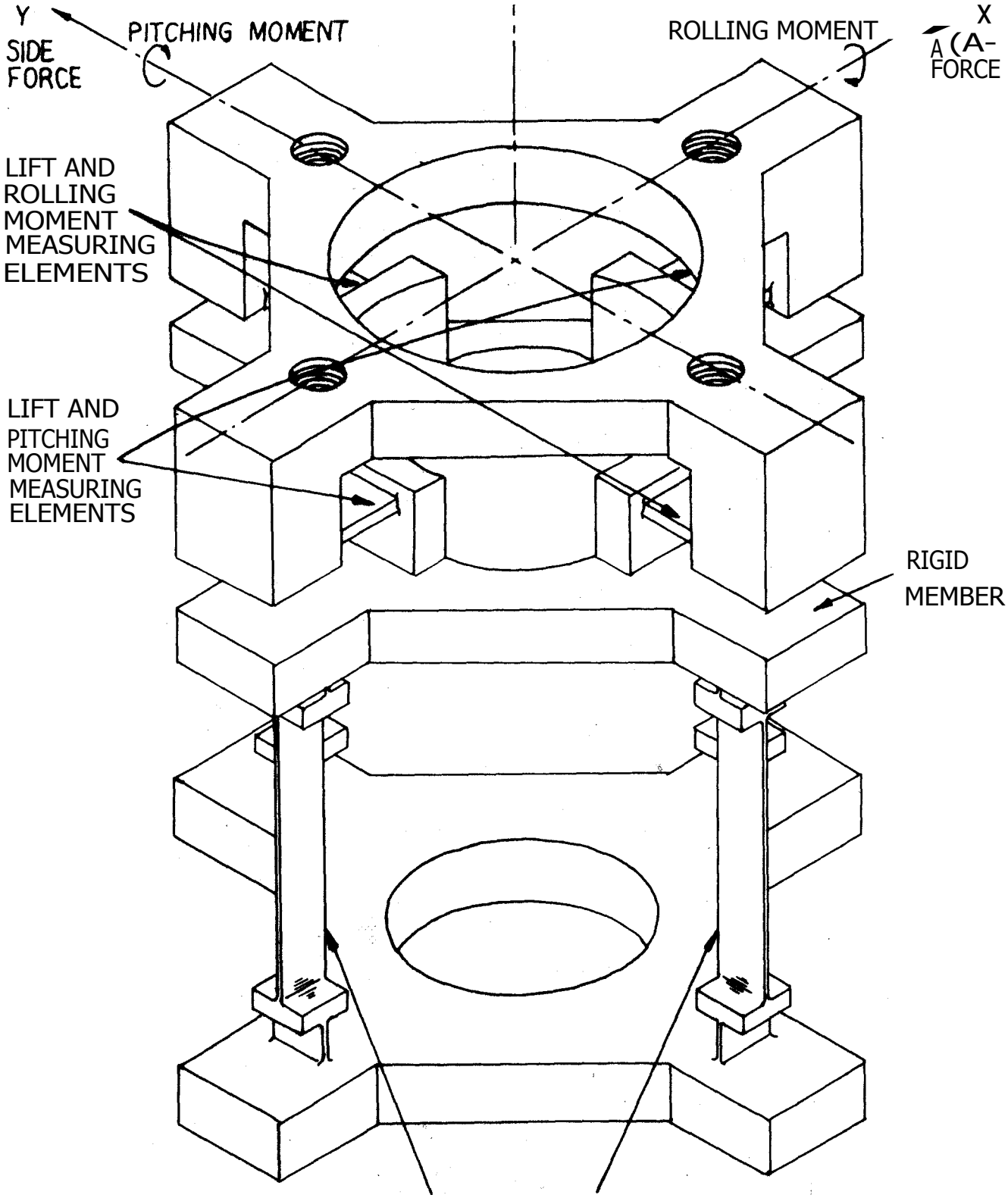

FIG. 4 ISOMETRIC VIEW OF THE ROTOR BALANCE

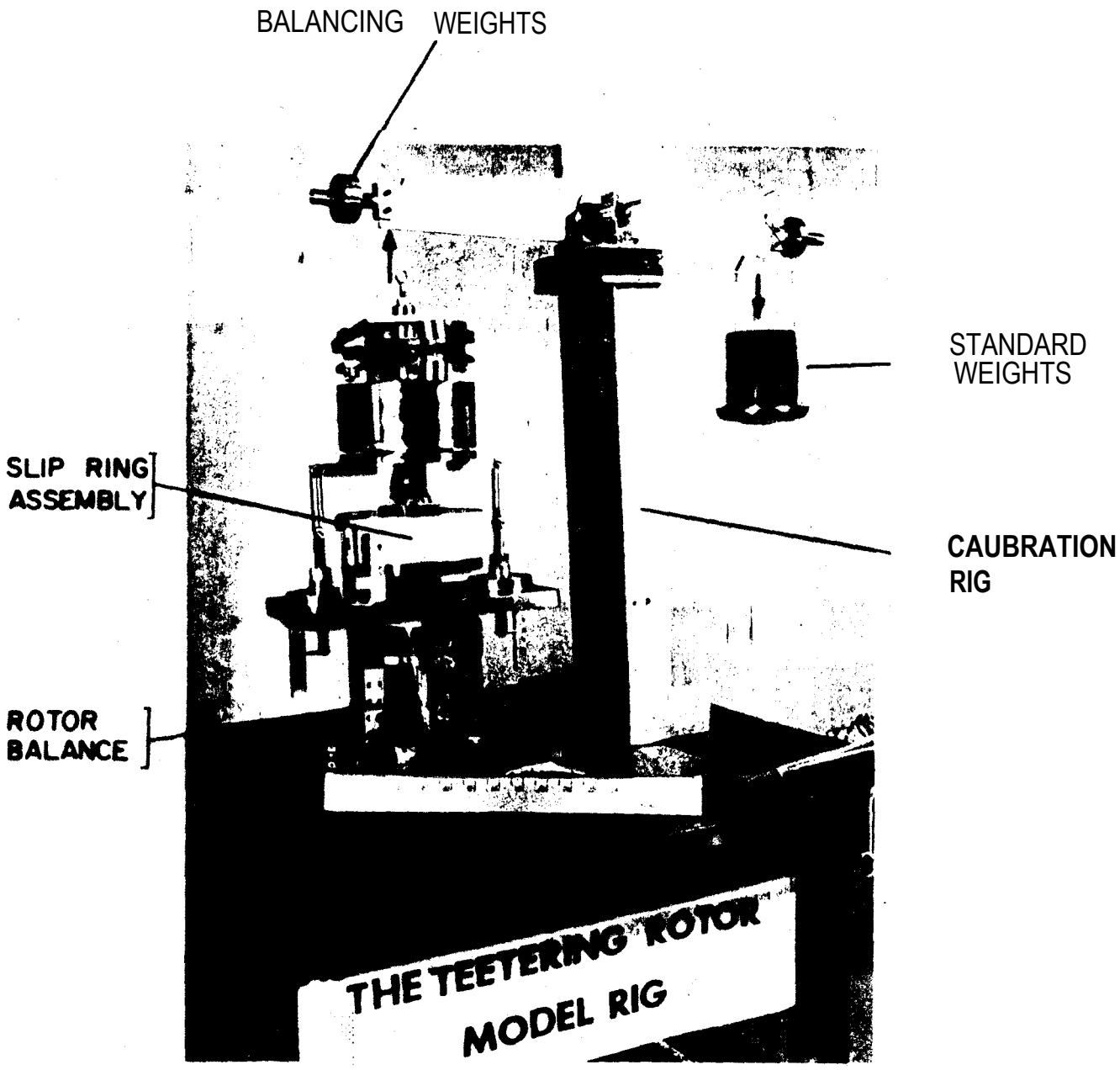

FIG. 5 CALIBRATION SET UP FOR LOADING LIFT FORCE (LOADING IN POSITIVE DIRECTION)

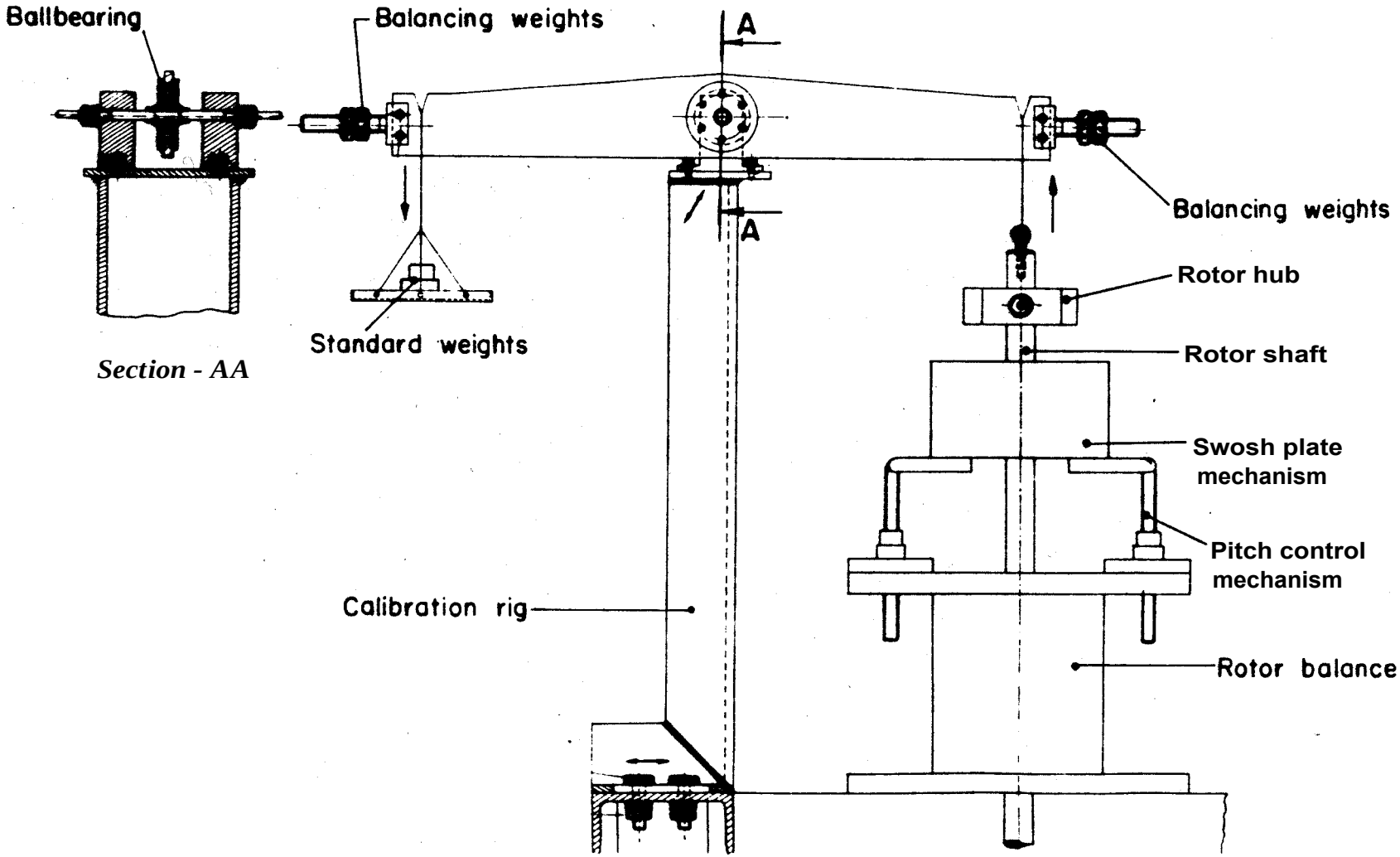

FIG. 6. **SCHEMATIC OF CALIBRATION RIG FOR LIFT FORCE**

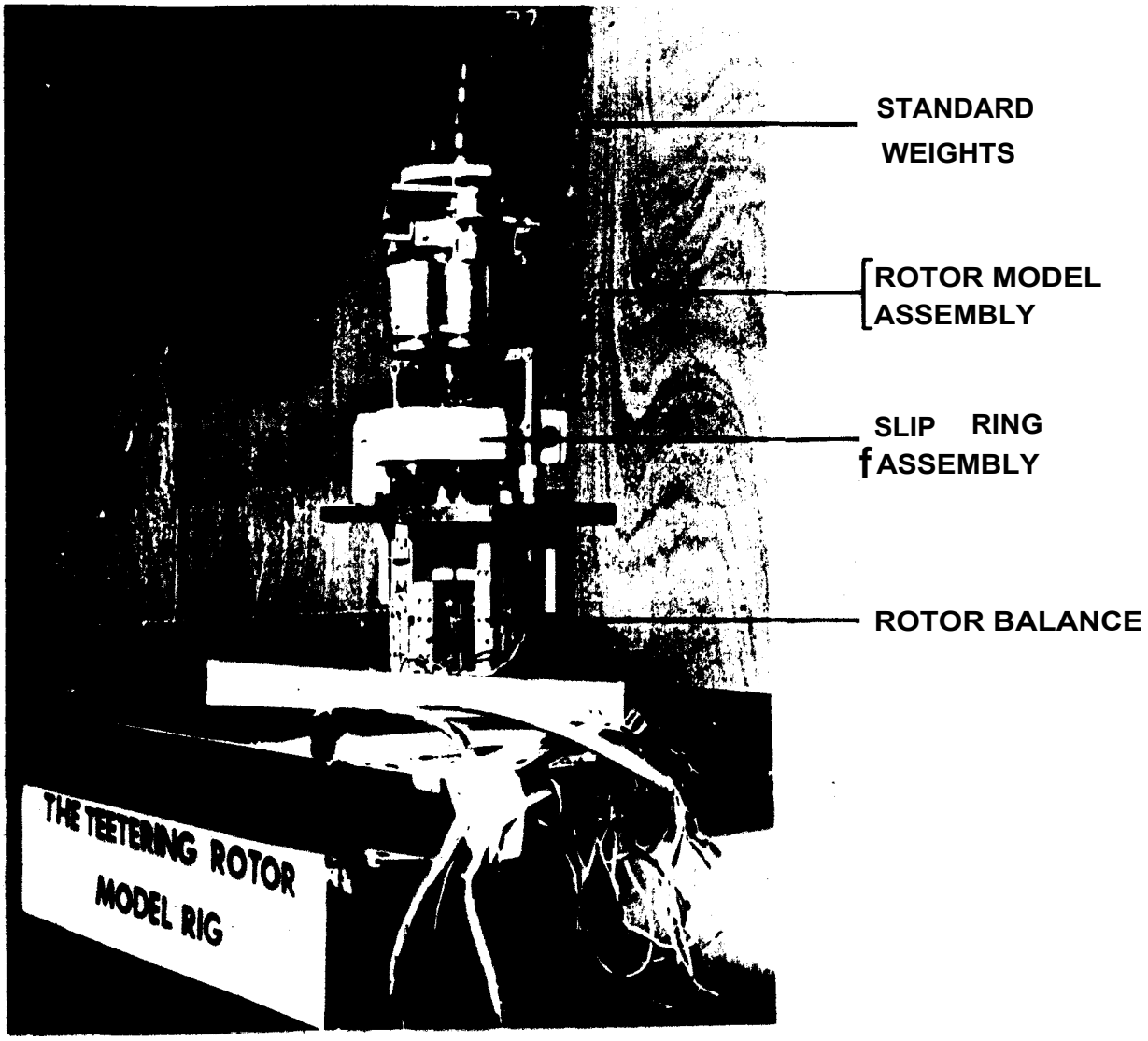

FIG. 7 LOADING FOR LIFT FORCE IN NEGATIVE DIRECTION

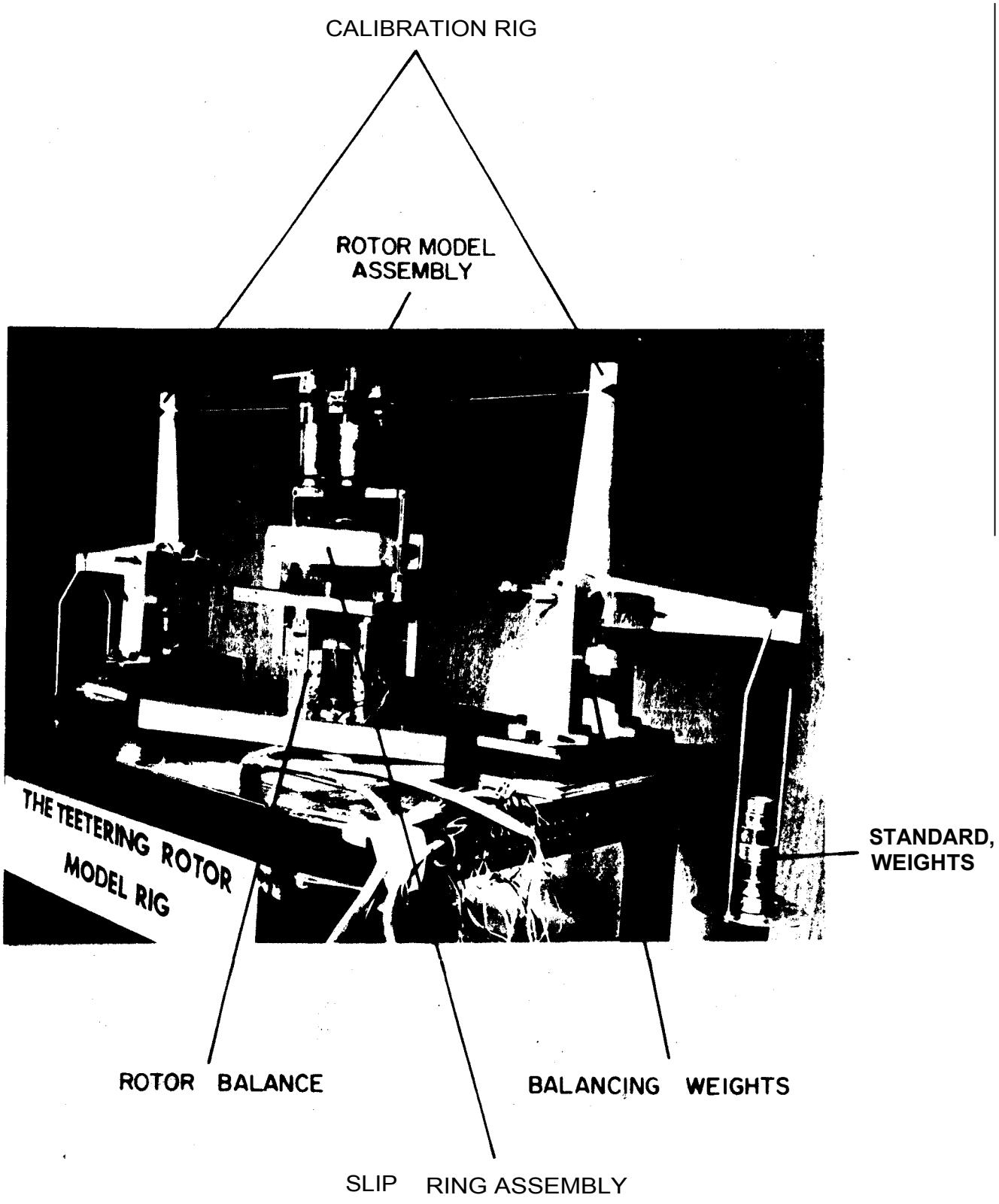

FIG. 8 SET UP FOR CALIBRATING PITCHING MOMENT, ROLLING MOMENT, DRAG FORCE & SIDE FORCE

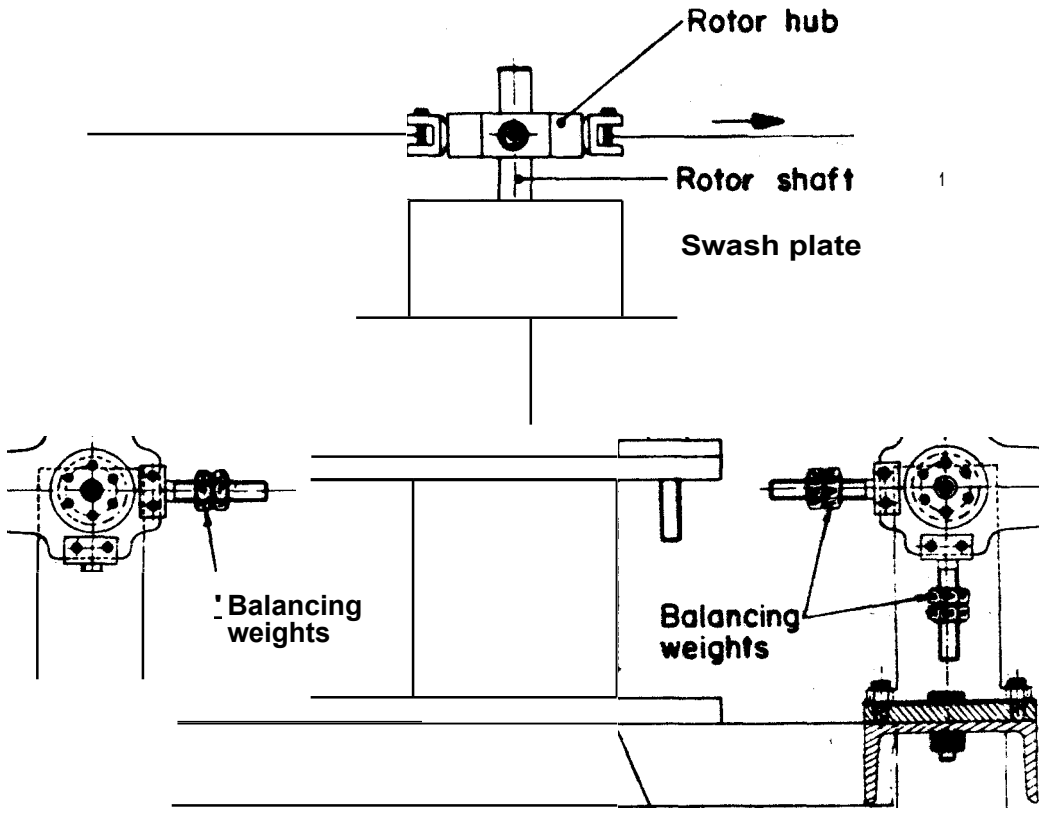

FIG.9. SCHEMATIC OF CALIBRATION RIG FOR PITCHING MOMENT_s ROLLING MOMENTS DRAG FORCE AND SIDE FORCE

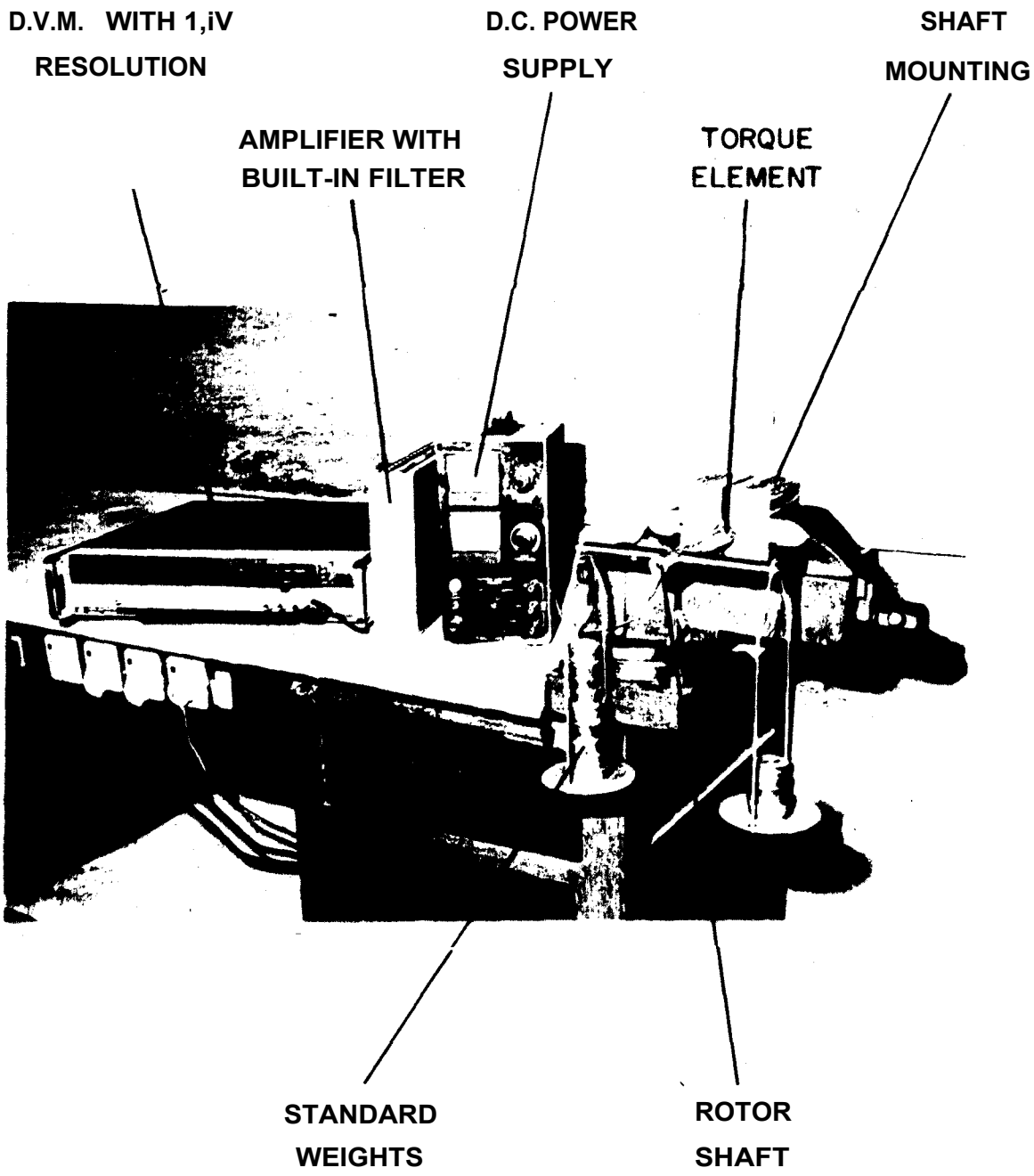

FIG. 10 CALIBRATION . SET- UP FOR STRAIN GAUGE TORQUE ELEMENT ON THE ROTOR SHAFT

Excitation voltage 3 V D.C

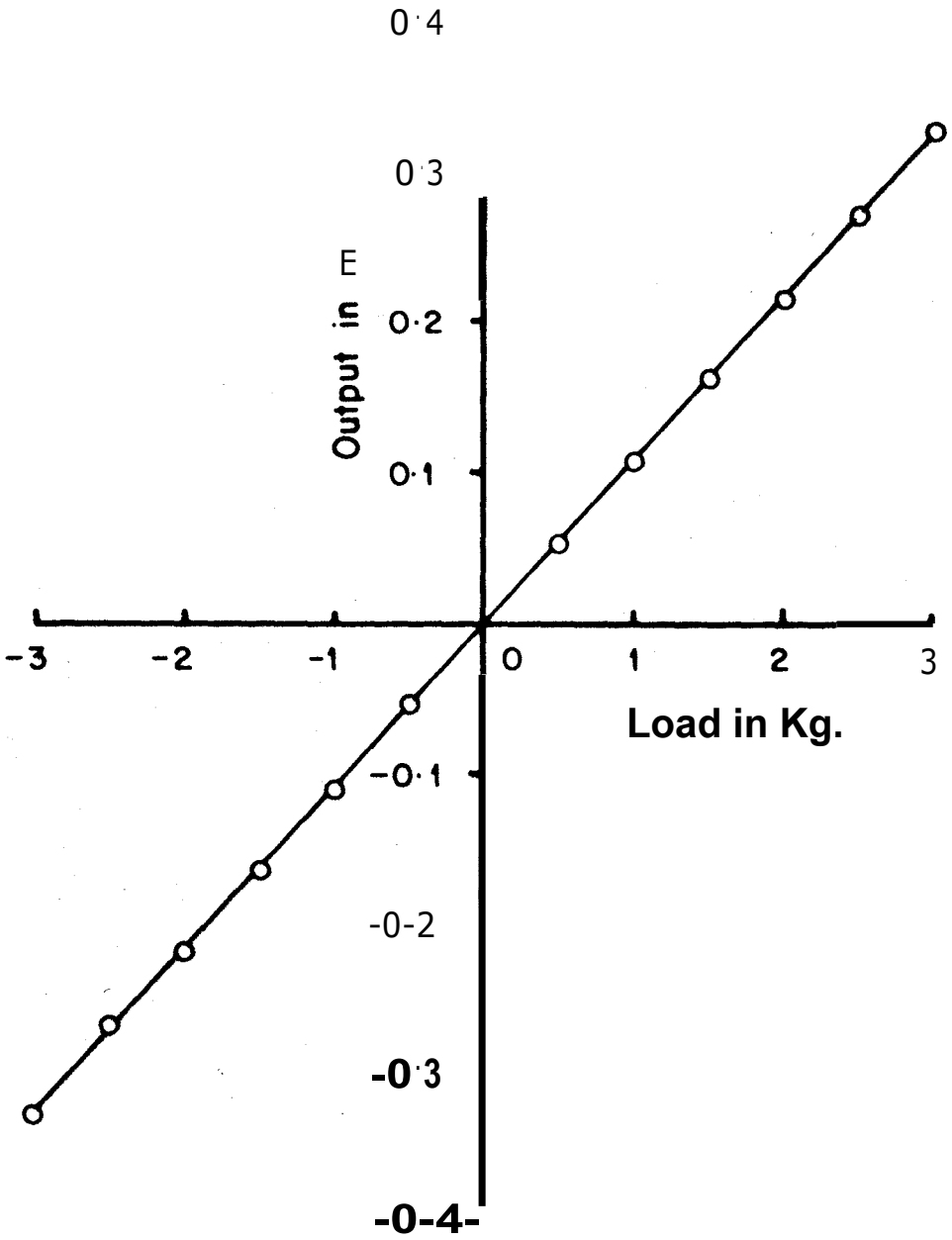

FIG.11. CALIBRATION CURVE FOR LIFT FORCE

Excitation voltage 3V. D.C

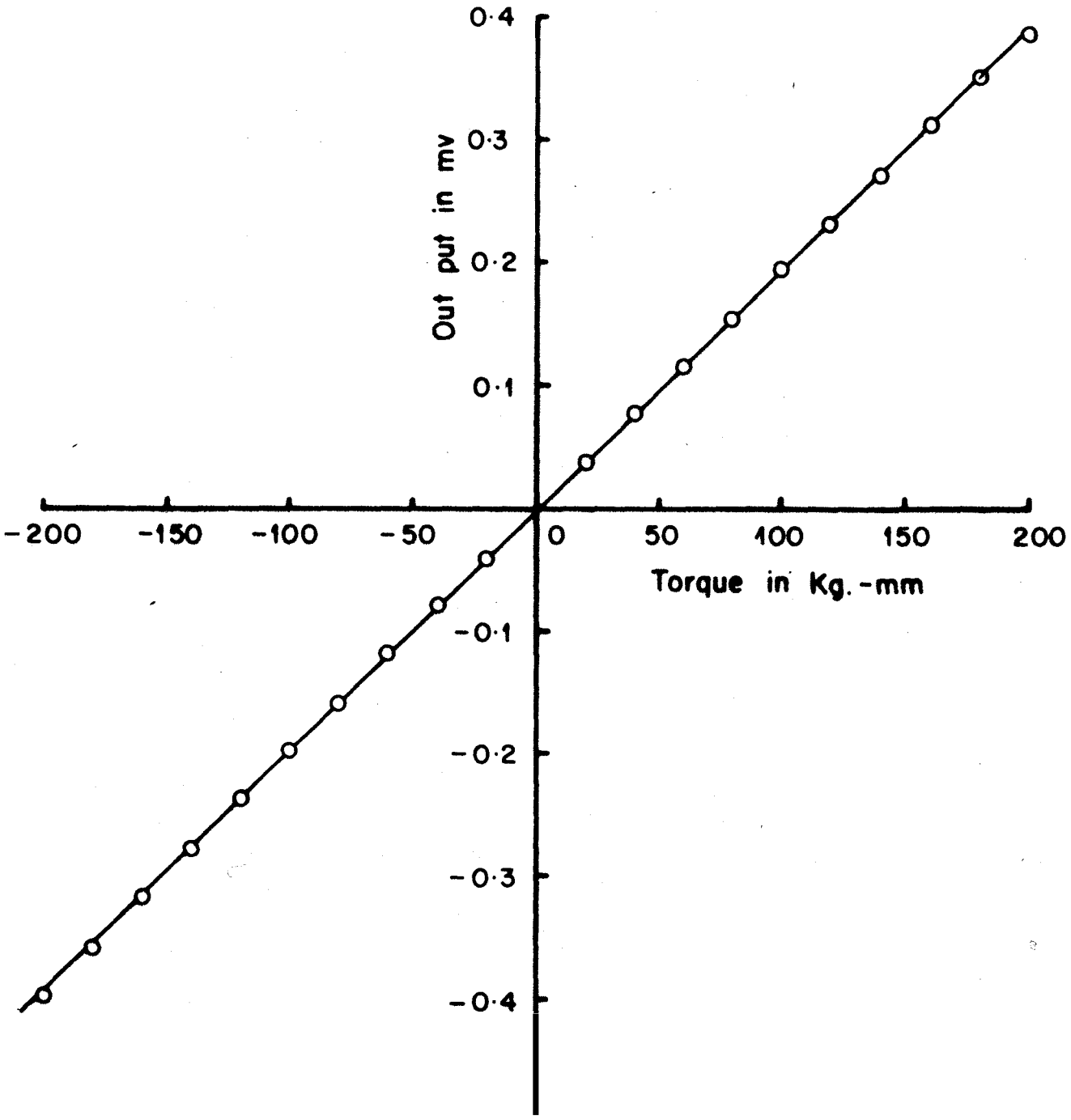

FIG. 12. CALIBRATION CURVE FOR TORQUE

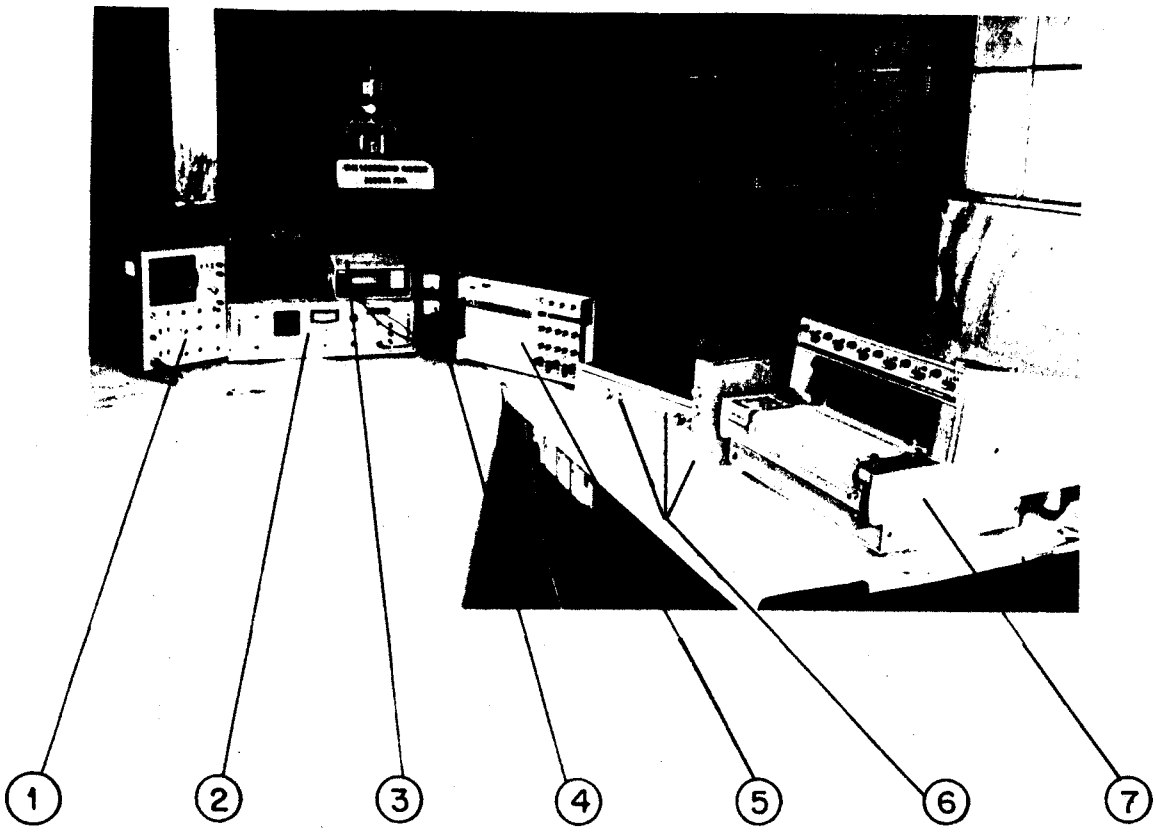

1 OSCILLOSCOPE

2 SPEED CONTROLLER WITH FEEDBACK SYSTEM

3 D.V.M. WITH ONE MICRO-VOLT RESOLUTION

4 D. C. POWER SUPPLY UNIT

5 OSCILLOGRAPH RECORDER

6 AMPLIFIERS WITH BUILT-IN FILTERS

7 STRIP CHART RECORDER

FIG. 13. MODEL ROTOR HOVER FACILITY

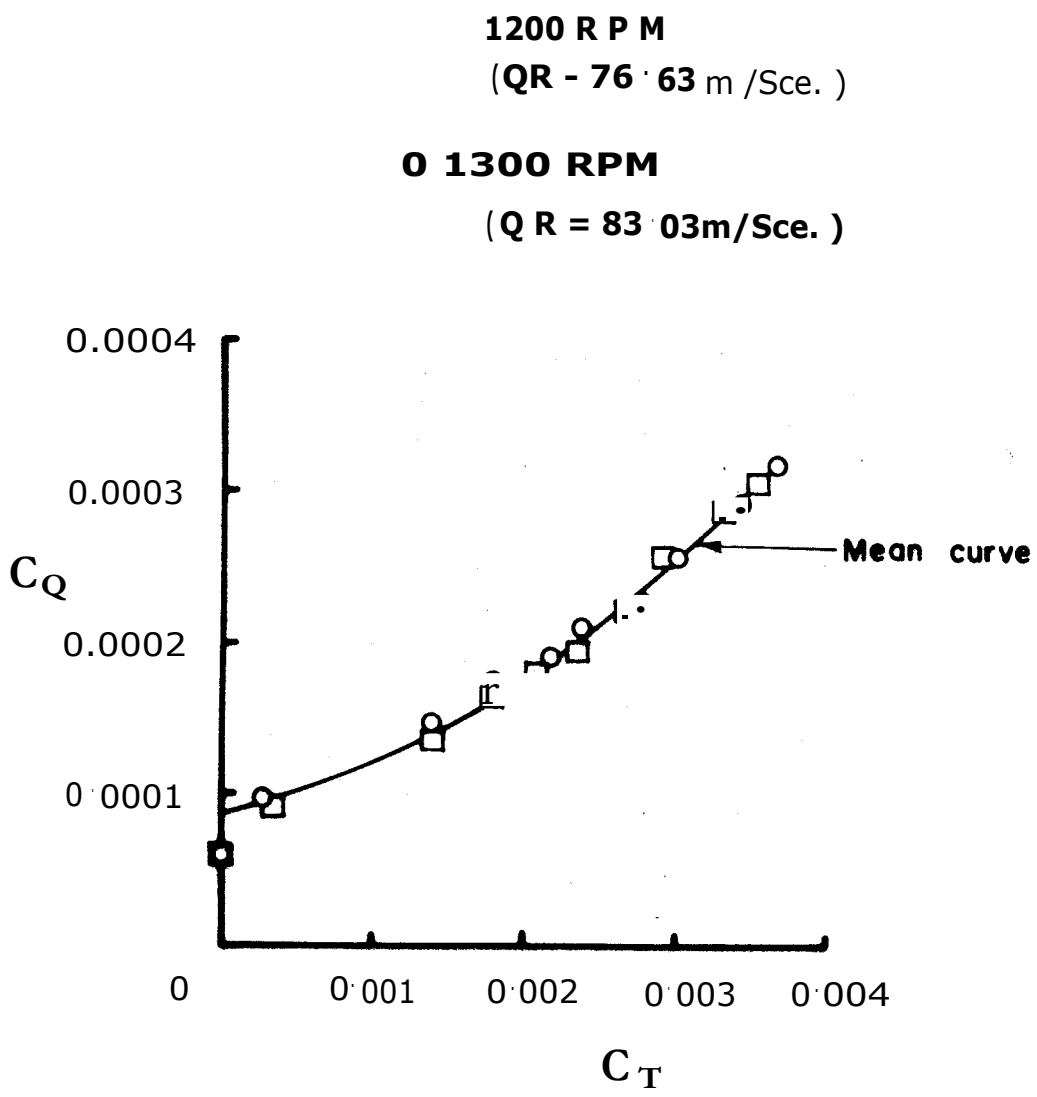

FIG.14. VARIATION OF ROTOR TORQUE COEFFICIENT WITH THRUST COEFFICIENT FOR ROTORAODEL OF OIA. 1.22-

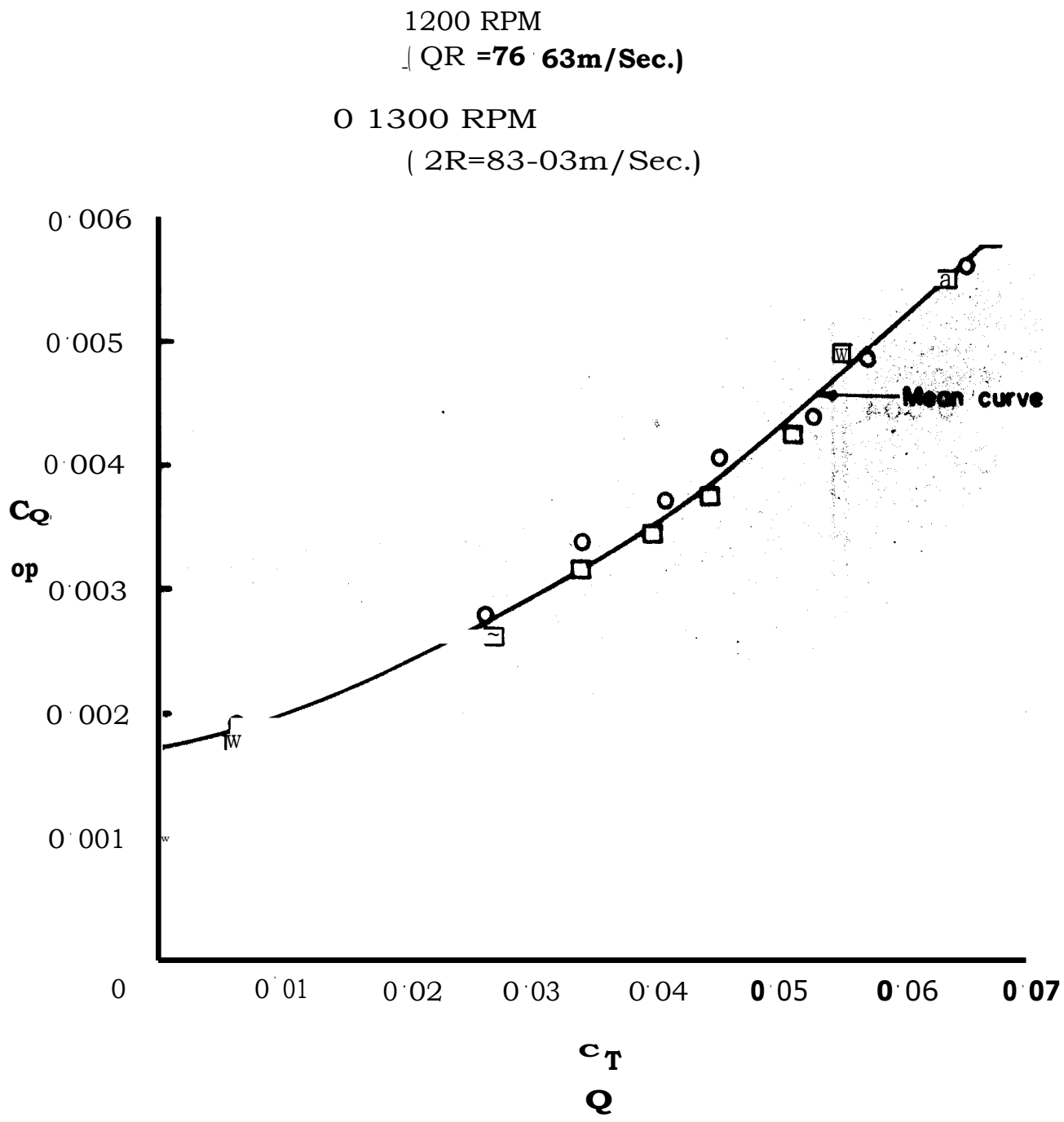

FIG. 15. HOVER POLAR FOR THE ROTOR MODEL OF DIA. 1.22m.

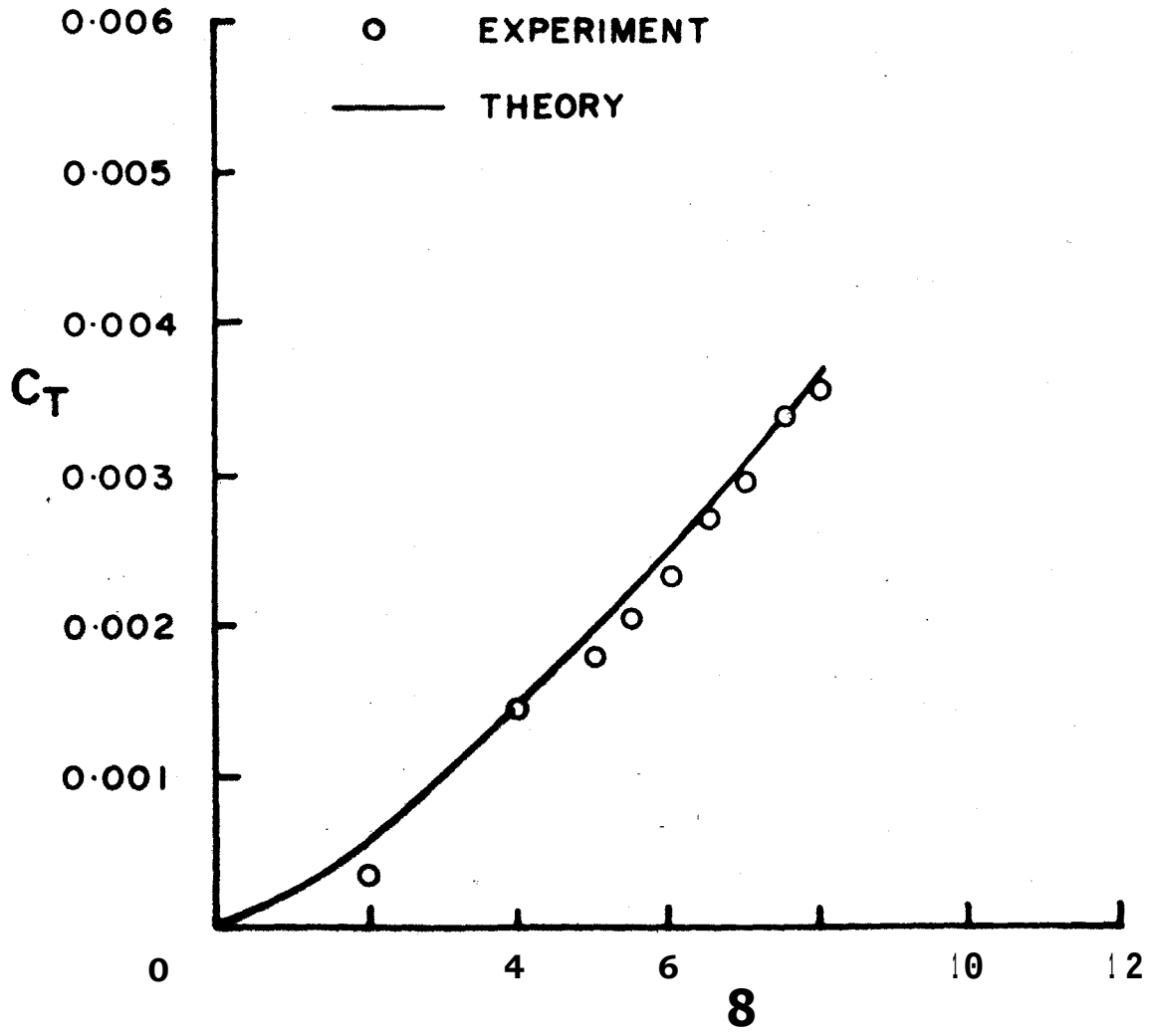

FIG. 16. VARIATION OF THRUST COEFFICIENT WITH COLLECTIVE PITCH FOR DIA.,1.22k ROTOR

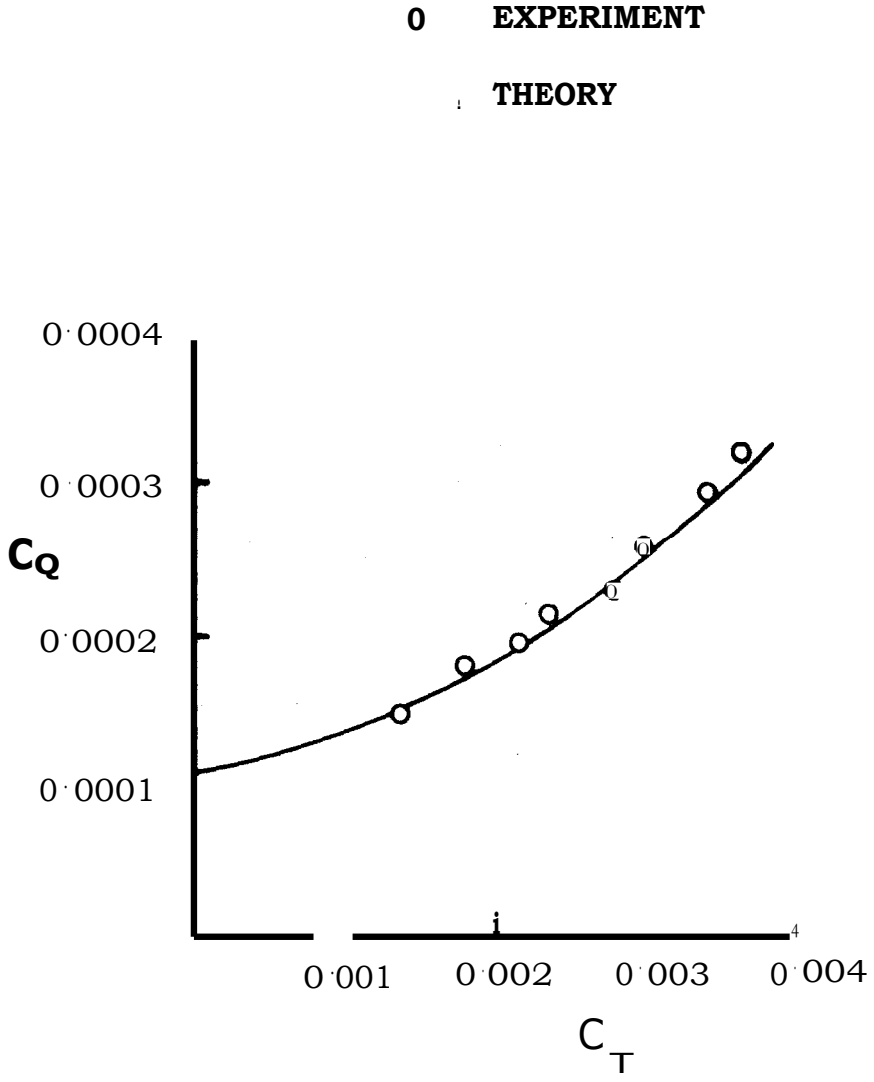

"IG.17. COMPARISION OF EXPERIMENTAL AND THEORETICAL HOVERING DATA OF ROTOR MODEL WITH CONSTANT CHORDS UNTWISTED BLADES

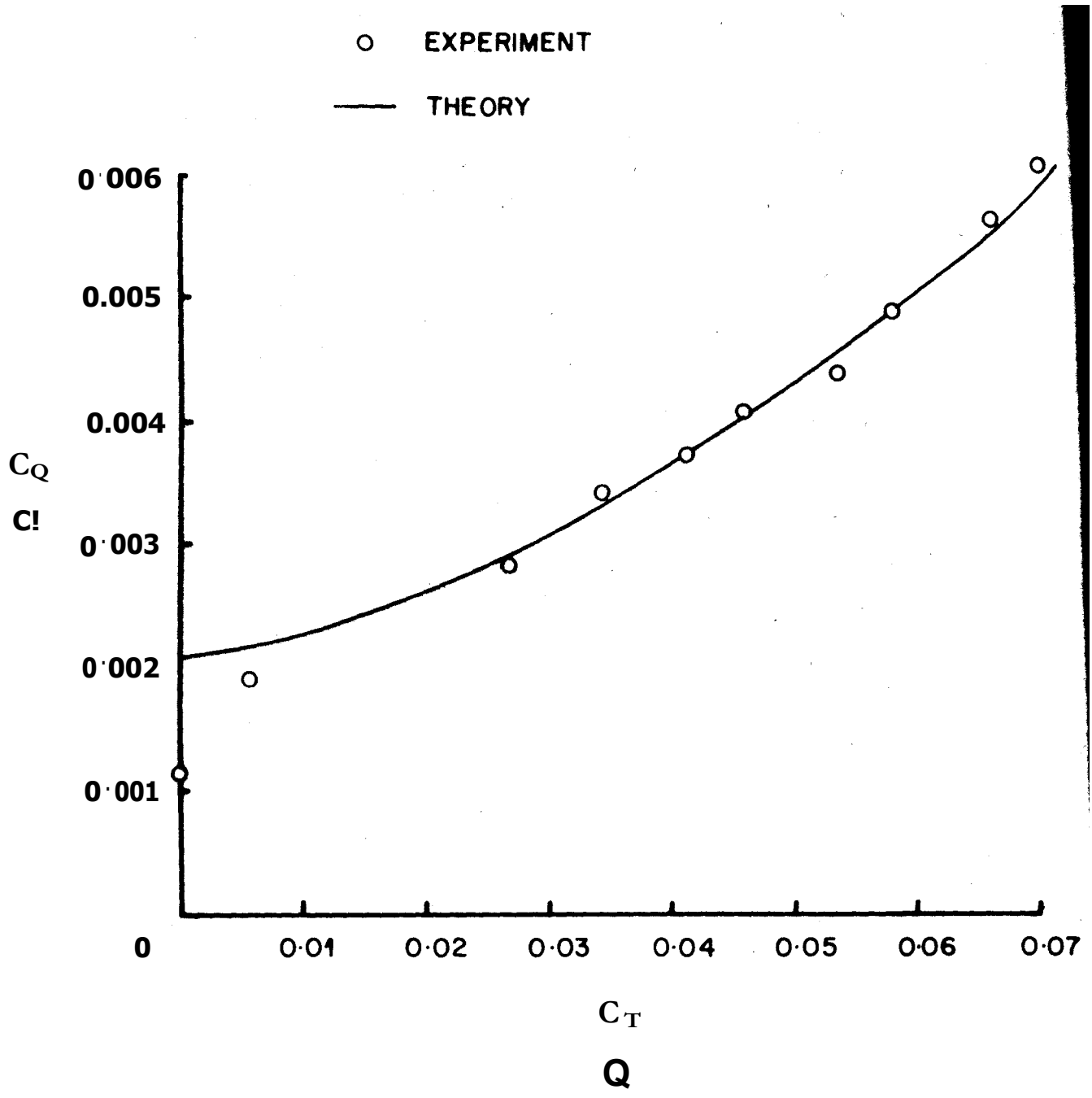

FIG.1$. COMPARISON OF EXPERIMENTAL AND THEORETICAL HOVER POLARS FOR DIA. 1.22k. ROTOR MODEL

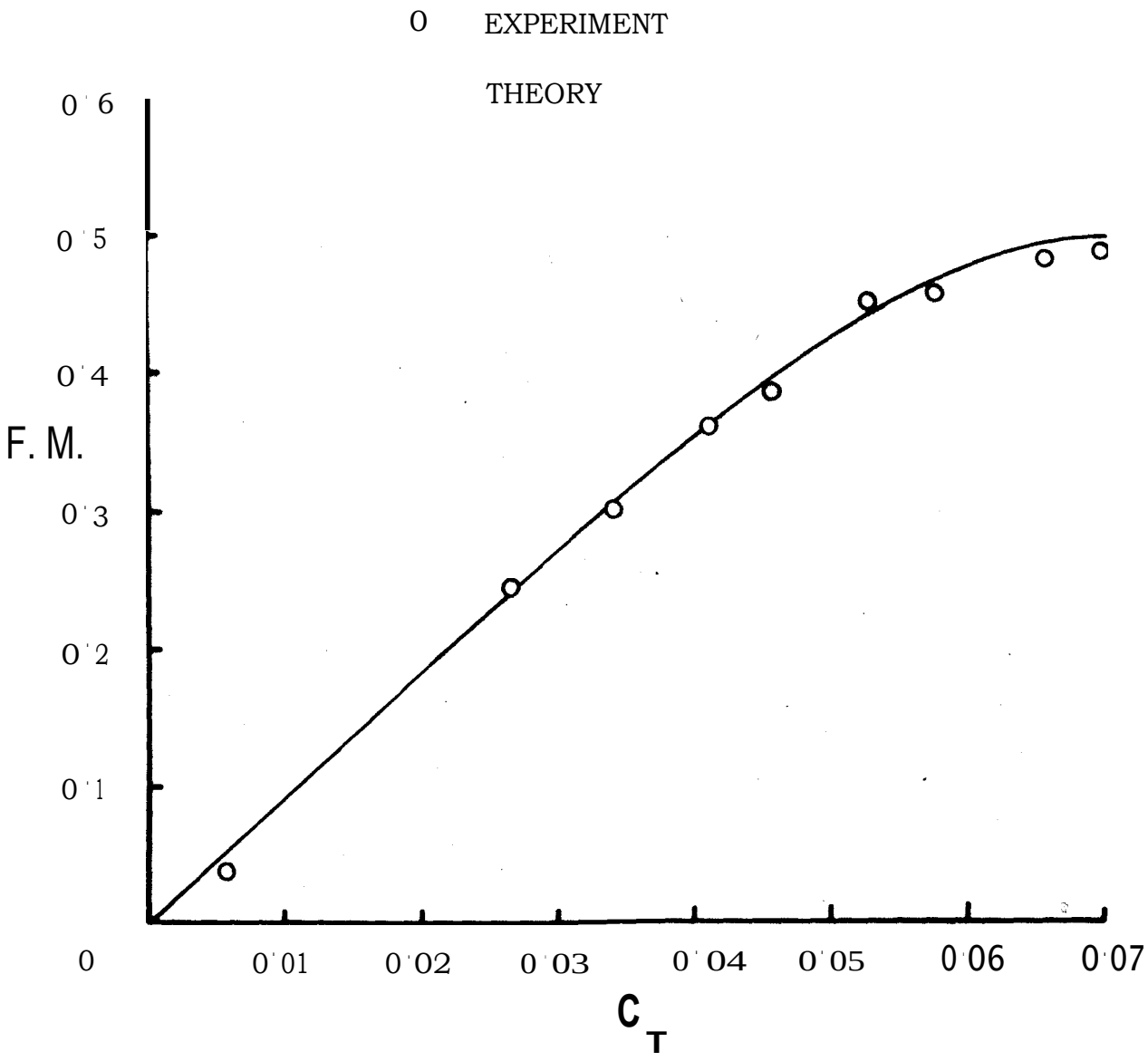

FIG.19. FIGURE OF MERIT. F.M. Vs CT/ (r - **COMPARISON OF EXPERIMENTAL AND THEORETICAL RESULTS OF DIA. 1.22.. ROTOR MODEL**

National Aeronautical Laboratory	Uocurnent *Classification* Unrestricted
Tit la MODEL HELICOPTER ROTOR RIG AND ASSOCIATED STRAINGAUGE BALANCE FOR PERFORMANCE STUDIES	Document No. TM AE 8704 *Date* of issue: August 1987
Author(s) S.R. PATIL, M.A. RAMASWAMY	Contents 31 pages Text: 12 Figures: 19
Division Aerodynamics	No. of copies: 30
External participation	*NAL Project No.*
Sponsor	*Sponsor's Project No.* AE-1-154
Approval Head, Aerodynamics Division	
Remarks	
Keywords Helicopter Rotor model, Hover Performance, Rotor Balance, Teetering Rotor	

Abstract

The details of teetering rotor model and the associated strain gauge balance and calibration fixtures have been presented.

Hovering results for 1.22m diameter teetering rotor model evaluated experimentally have been compared with the simple blade element momentum theory.